

Article

A Hydrothermal Synthesis Process of ZSM-5 Zeolite for VOCs Adsorption Using Desilication Solution

Zhenhua Sun^{1,2}, Qingxiang Shu³, Qikun Zhang³ , Shaopeng Li², Ganyu Zhu², Chenye Wang^{2,*}, Jianbo Zhang², Huiquan Li^{2,4} and Zhaohui Huang^{1,*}

¹ School of Materials Science and Technology, China University of Geosciences (Beijing), Beijing 100083, China; zhsun@ipe.ac.cn

² CAS Key Laboratory of Green Process and Engineering, National Engineering Research Center of Green Recycling for Strategic Metal Resources, Institute of Process Engineering, Chinese Academy of Sciences, Beijing 100190, China; shpli@ipe.ac.cn (S.L.); gyzhu@ipe.ac.cn (G.Z.); zhangjianbo@ipe.ac.cn (J.Z.); hqli@ipe.ac.cn (H.L.)

³ School of Chemistry and Material Science, Shandong Normal University, Jinan 250014, China; shuqingxiang@ipe.ac.cn (Q.S.); zhangqk@sdnu.edu.cn (Q.Z.)

⁴ School of Chemical Engineering, University of Chinese Academy of Sciences, Beijing 100049, China

* Correspondence: cywang@ipe.ac.cn (C.W.); huang118@cugb.edu.cn (Z.H.)

Abstract: ZSM-5 zeolite is a kind of high-value-added porous aluminosilicate zeolite. The use of the coal gasification slag utilization process by-product desilication liquid as a silicon raw material to replace the current raw materials such as water glass will help reduce production costs and achieve high-value utilization of solid waste. ZSM-5 zeolites for volatile organic compounds (VOCs) adsorption were prepared by a one-step hydrothermal method using the desilication solution prepared from coal gasification slag as the main silicon source and sodium source. The effects of crystallization reaction time, the crystallization temperature, the Na₂O/SiO₂ molar ratio, and the SiO₂/Al₂O₃ molar ratio on the relative crystallinity and the specific surface area of the ZSM-5 zeolite were investigated and optimized. The optimal reaction conditions were as follows: a crystallization time of 12 h, a crystallization temperature of 170 °C, a Na₂O/SiO₂ molar ratio of 0.2, and a SiO₂/Al₂O₃ molar ratio of 200. The optimal ZSM-5 zeolite synthesized is hexagonal, with regular grains, a relative crystallinity of 101.48%, a specific surface area of 337.48 m²·g⁻¹, and a pore volume of 0.190 cm³·g⁻¹. And the optimal ZSM-5 zeolite was composed of SiO₂ content of 97.52 wt%, Al₂O₃ content of 1.58 wt%, Na₂O content of 0.33 wt%, and SiO₂/Al₂O₃ molar ratio of 104.93. Na₂O/SiO₂ molar ratio is 0.0033. The results of static adsorption experiments show that the static adsorption capacities of ZSM-5 zeolite for *p*-xylene, benzene, toluene, and butyl acetate were 118.85, 69.98, 68.74, and 95.85 mg·g⁻¹, respectively, which can effectively adsorb VOCs. The synthetic process of the ZSM-5 zeolite is a simple preparation process and short in synthesis time. The results of this study not only help to realize the high-value utilization of silicon components in solid waste, but also provide an economical and effective way to synthesize VOCs adsorption materials.

Keywords: ZSM-5 zeolite; hydrothermal synthesis; adsorption; volatile organic compounds



Citation: Sun, Z.; Shu, Q.; Zhang, Q.; Li, S.; Zhu, G.; Wang, C.; Zhang, J.; Li, H.; Huang, Z. A Hydrothermal Synthesis Process of ZSM-5 Zeolite for VOCs Adsorption Using Desilication Solution. *Separations* **2024**, *11*, 39. <https://doi.org/10.3390/separations11020039>

Academic Editor: Ki Hyun Kim

Received: 26 December 2023

Revised: 13 January 2024

Accepted: 24 January 2024

Published: 26 January 2024



Copyright: © 2024 by the authors. Licensee MDPI, Basel, Switzerland. This article is an open access article distributed under the terms and conditions of the Creative Commons Attribution (CC BY) license (<https://creativecommons.org/licenses/by/4.0/>).

1. Introduction

ZSM-5 is an aluminosilicic and pentasilicic zeolite composed of silicon (Si⁴⁺) and aluminum ions (Al³⁺), which are surrounded by four oxygen anions (O²⁻) [1]. ZSM-5 zeolite is a five-membered ring structure composed of [SiO₄] tetrahedron and [AlO₄] tetrahedron connected by an oxygen atom with a common vertex [2], which has a MFI-type structure [3]. ZSM-5 zeolite is a kind of porous zeolite with a high content of silicon five-membered ring structures. The internal pore structure of ZSM-5 zeolite is a special three-dimensional channel composed of a straight hole of a ten-membered ring and another zigzag ten-membered ring hole [4]. ZSM-5 zeolites are usually used in petroleum refining [5] and chemical

engineering [6] due to their good shape selectivity, high ion exchange performance, good hydrophobicity, excellent acid resistance, and good thermal stability [7]. With the development of the environmental protection industry, the application of ZSM-5 zeolite has gradually expanded to the efficient adsorption [8] of volatile organic compounds (VOCs) due to its non-flammability [9], excellent moisture resistance, and good recycling [10]. The synthesis methods of ZSM-5 zeolites mostly use sodium silicate, silica sol, and other raw materials. There are high material costs, long reaction times, and other problems, so it is necessary to explore a new process with low raw materials costs, short reaction times, and green synthesis methods.

Coal gasification slag is a kind of main aluminosilicate solid waste produced by incomplete combustion during coal gasification reactions [11]. In recent years, China's annual emissions of coal gasification slag continue to grow [12]. However, stacking [13] and land-filling [14] as the main treatment methods pose a serious threat to land resources and the ecological environment [15]. Qu et al. [16] prepared coal gasification slag desilication liquid through acid activation and alkali desilication by taking advantage of the characteristics of rich SiO_2 and Al_2O_3 in coal gasification slag. The main elements of the solute in the desilication solution are Si and Na, which contain trace metal impurities. And it is a very good potential silicon raw material for zeolite synthesis.

The hydrothermal method, as a simple and convenient method for preparation, has been widely used in the industrial production of zeolite [17]. At present, the one-step hydrothermal process of ZSM-5 zeolite is mainly the "aging hydrothermal crystallization" process [18], with aging and a crystallization time usually greater than 24 h [19]. In this paper, the desilication solution was prepared by acid activation and alkali desilication of coal gasification slag, which was used as the main silicon source and sodium source. After mixing with an aluminum source, the template agent and the ZSM-5 zeolite seed without an aging step, the ZSM-5 zeolite for removing VOCs was prepared by controlling the temperature and time of hydrothermal crystallization and the ratio of Na_2O and SiO_2 in the precursor. The network structure of SiO_2 in the desilication solution is beneficial to the rapid nucleation and crystal growth of ZSM-5 zeolite. At the same time, through the structural guidance of the template agent, the time of hydrothermal crystallization synthesis is reduced to achieve the goal of the rapid synthesis of a microporous ZSM-5 molecular sieve with stability, a good specific surface area and high crystallinity. The crystal properties of ZSM-5 zeolite prepared under different synthesis conditions were investigated by various characterization methods such as N_2 adsorption and desorption, X-ray diffraction spectroscopy, and scanning electron microscopy. The effects of reaction conditions on the relative crystallinity and the specific surface area were systematically investigated, and the adsorption performance of ZSM-5 zeolite was evaluated. The preparation process of this article is simple, utilizing the synthesized ZSM-5 zeolite to adsorb VOCs, while also achieving high-value utilization of solid waste, effectively reducing costs, and exploring a green synthesis process for ZSM-5 zeolite.

2. Experimental

2.1. Materials

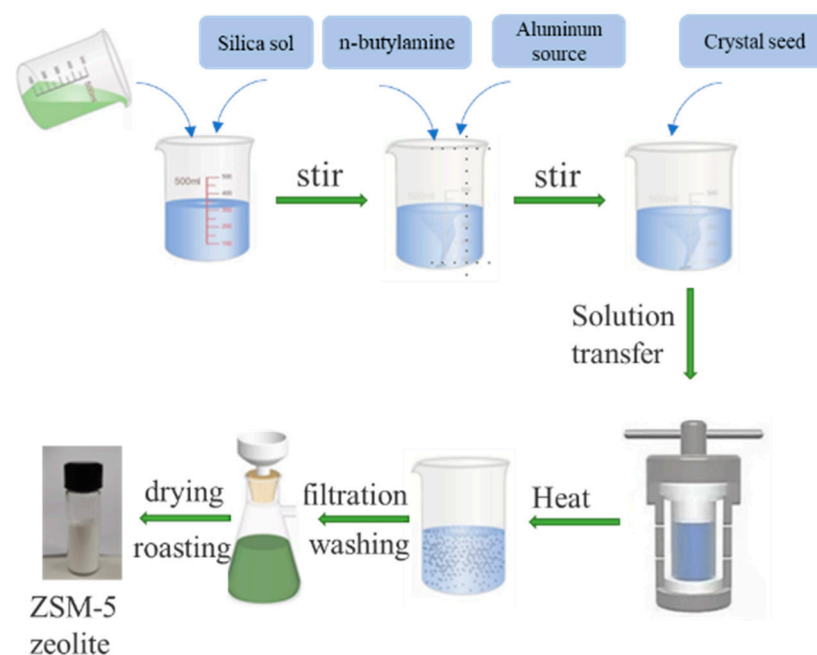
The preparation method of the desilication solution comes from the previous research of our research team [16], which is prepared from coal gasification slag as the silicon-containing raw material. The element concentration of the desilication solution is shown in Table 1. Hydrochloric acid (HCl, AR), aluminum sulfate octahydrate ($\text{Al}_2(\text{SO}_4)_3 \cdot 18 \text{H}_2\text{O}$, AR) and sodium hydroxide (NaOH, AR) are all purchased from China National Pharmaceutical Chemical Reagent Co., Ltd., Shanghai City, China. Silica sol (SiO_2 , 29–31 wt%, AR) and n-butylamine ($\text{C}_4\text{H}_{11}\text{N}$, GC) were purchased from McLean Biochemical Technology Co., Ltd., Shanghai City, China. ZSM-5 zeolite seeds, p-xylene (C_8H_{10} , AR), benzene (C_6H_6 , AR), toluene (C_7H_8 , AR), and butyl acetate ($\text{C}_6\text{H}_{12}\text{O}_2$, AR) were all purchased from Shanghai Aladdin Biochemical Technology Co., Ltd. Shanghai City, China.

Table 1. Concentration of each element of desilication solution.

Elements	Si	Al	Na
Concentration/(g·L ⁻¹)	74.03	0.49	35.65

2.2. Synthesis of ZSM-5 Zeolite

The initial molar composition of the raw material designed for the preparation of ZSM-5 zeolite is $\text{SiO}_2:\text{Al}_2\text{O}_3:\text{Na}_2\text{O}:\text{H}_2\text{O}:\text{n-butylamine} = 1:x(0.02\sim 0.0001):(0.05\sim 0.4):30:0.4$, and the mass of the seed is 4% of the total mass of SiO_2 . The hydrothermal synthesis process of ZSM-5 zeolite is shown in Figure 1. The composition design was carried out according to the known chemical composition of the desilication solution. When $x = 0.005$, $y = 0.2$, 25 mL concentrated desilication liquid of coal gasification slag was measured, and 10.8 g silica sol was added to it. After stirring well, 0.368 g NaOH and 3.5 g n-butylamine were added and stirred for 30 min, as a silicon solution. Then, 0.25 g $\text{Al}_2(\text{SO}_4)_3 \cdot 18 \text{H}_2\text{O}$, ultrapure water was mixed as the aluminum solution, and was added to the silicon solution drop by drop. The 0.29 g ZSM-5 zeolite seeds was used to accelerate the crystallization reaction. The emulsion gel was stirred for 30 min to be used as the reaction precursor. Finally, the mixture was poured into a 100 mL hydrothermal reactor and heated in a homogeneous reactor. The suspension after crystallization was filtered, washed to a neutral pH value, and then dried at 110 °C for 12 h. The ZSM-5 zeolite product was prepared by calcining the dried sample at 550 °C for 6 h to remove the template in a muffle furnace.

**Figure 1.** The hydrothermal synthesis process of ZSM-5 zeolite.

2.3. Characterization and Analysis Methods

Inductively coupled plasma spectrometry (ICP-OES, Avio200, PerkinElmer, Waltham City, MA, USA) was used to detect the concentration of Si, Al, and Na elements in the desilication solution, with the wavelength range of 165–782 nm (± 0.1 nm). Through powder X-ray diffraction (XRD, Empyrean, PANalytical B.V., Almelo, The Netherlands.) to determine the product phase structure, the voltage is 40 kV, the current is 40 mA, the $\text{Cu K}\alpha$ radiation source has a 2θ range of 5–45° ($\lambda = 0.15406$ nm), the scanning rate is 4°/min, and the step size is 0.02°. The relative crystallinity of ZSM-5 zeolite is determined by comparing the sum of characteristic peak areas. A 600M liquid nuclear magnetic resonance spectrometer (NMR, Bruker AVANCE III, Bruker Corporation, Salbrücken, Germany) was used to

determine ^{29}Si in the desilication solution of coal gasification slag. At room temperature, the magnetic field strength was 14.09 T, and D_2O was used as the solvent. Use an X-ray fluorescence spectrometer (XRF) to determine the chemical composition of the sample, with a test voltage and current of 50 kV and 60 mA, respectively. N_2 physical adsorption was measured at 77 K using a fully automated surface area and micropore analyzer (BET, ASAP 2020 PlusHD88, Mack Instruments, Norcross, GA, USA). The samples were analyzed after vacuum degassing at 350 °C for 6 h. The specific surface area (SBET) is determined by the Brunauer–Emmett–Teller (BET) equation. When the relative pressure is 0.99, the total pore volume (V_{pore}) is obtained according to the nitrogen storage capacity. The pore size distribution was calculated based on the Barret–Joyner–Halenda (BJH) method. The morphologies of the products were tested by scanning electron microscopy (SEM, JSM-7800 (Prime), JEOL Japan Electronics Co., Ltd., Tokyo, Japan). The ZSM-5 zeolite sample was ultrasonically dispersed with anhydrous ethanol and then dropped onto a copper mesh to dry naturally. The morphology and elements distribution of the sample were analyzed by transmission electron microscopy (TEM, JEM-F200, JEOL Japan Electronics Co., Ltd., Tokyo, Japan), high-resolution transmission electron microscopy (HR-TEM), energy dispersive spectroscopy (EDS), and selected area electron diffraction (SAED) on the field emission transmission electron microscope. The functional group structure of ZSM-5 zeolite at wavelengths of 400–4000 cm^{-1} was obtained by Fourier transform infrared spectroscopy (FT-IR, Tensor27, Bruker Corporation, Salbrücken, Germany).

2.4. The Adsorption Testing Method

First, 150 mg ZSM-5 zeolite samples was weighed with a balance and roasted at 550 °C in a Muffle furnace for 1 h to remove water and other organic impurities. Then, the ZSM-5 zeolite was accurately weighed into a weighing bottle and placed in a dryer with a beaker containing 100 mL of different organic solvents. After 24 h adsorption at 35 °C, the sample was taken out and weighed to calculate the adsorption capacity. The static adsorption capacity of the ZSM-5 zeolite sample for different VOCs is calculated according to the following equation:

$$q = \frac{(m_3 - m_2) * 10^3}{(m_2 - m_1)} \quad (1)$$

where q is the equilibrium adsorption capacity of ZSM-5 zeolite on VOCs, $\text{mg}\cdot\text{g}^{-1}$; m_1 is the weight of the measuring bottle, g; m_2 is the weight of the weighing bottle and the roasted ZSM-5 zeolite, g; m_3 is the weight of the weighing flask and the adsorbed ZSM-5 zeolite, g.

3. Results and Discussion

3.1. Effects of the Crystallization Reaction Time

The crystallization reaction processes of the samples mainly consist of an induction period and a grain growth period. The products during the induction period are in an amorphous state; and after a period of crystallization, zeolite crystals are rapidly generated. At this time, the products are in a metastable phase and can be transformed into other crystal phases. As the crystallization reaction progressed to the later stage, the crystal synthesis rate decreased, mainly because the concentration of silicate and meta-aluminate in the system gradually decreased. If the crystallization time is too short, the crystallization reaction in the system will be interrupted, which is not conducive to crystal growth, and the degree of crystallization of the product will be low. If the crystallization time is too long, it may cause the already crystallized products to transform into other types of zeolites, so the crystallization reaction time plays a crucial role in the synthesis of ZSM-5 zeolites. In order to study the effect of synthesis time on the crystallinity, the hydrothermal crystallization experiments were carried out for 6 h, 12 h, 24 h, 36 h, and 48 h under the conditions of a synthesis reaction temperature of 170 °C and the molar composition of $\text{SiO}_2:\text{Al}_2\text{O}_3:\text{Na}_2\text{O}:\text{H}_2\text{O}:\text{n-butyl amine} = 1:0.005:0.2:30:0.4$. The XRD patterns of the ZSM-5

zeolite samples under different crystallization times are shown in Figure 2a. The products generated within 6–48 h have obvious characteristic peaks at 7.9° , 8.8° , 23.0° , 23.9° , and 24.4° , which are ZSM-5 zeolite structures [20,21]. The results show that ZSM-5 zeolites can crystallize in a relatively wide time range. With the increase in reaction time, the diffraction peak intensity of ZSM-5 firstly increases and then decreases. When the crystallization time is 24–48 h, the quartz phase is formed gradually, and the peak intensity increases with time. Calculate and analyze the relative crystallinity of different products based on XRD results, as shown in Figure 2b. With the increase in time, the relative crystallinity of the ZSM-5 zeolite samples increases first and then decreases gradually. When the crystallization time is 6 h, the relative crystallinity of the product is 96.91%. When the hydrothermal crystallization time is 12 h, the relative crystallinity increases to 101.48%. It can be seen that the time required for the hydrothermal synthesis of ZSM-5 zeolite with the desilication liquid as the main raw material is far less than that of traditional hydrothermal synthesis. The network structure of SiO_2 in the desilication liquid is conducive to rapid nucleation and crystal growth of ZSM-5 zeolite. In addition, the time required for synthesis is greatly shortened through the structural guidance of the template. When the crystallization reaction time increased to 24 h, the relative crystallinity rapidly decreased to 81.42%. As time continued to extend, the relative crystallinity continued to decrease, and the product transformed into more quartz phases.

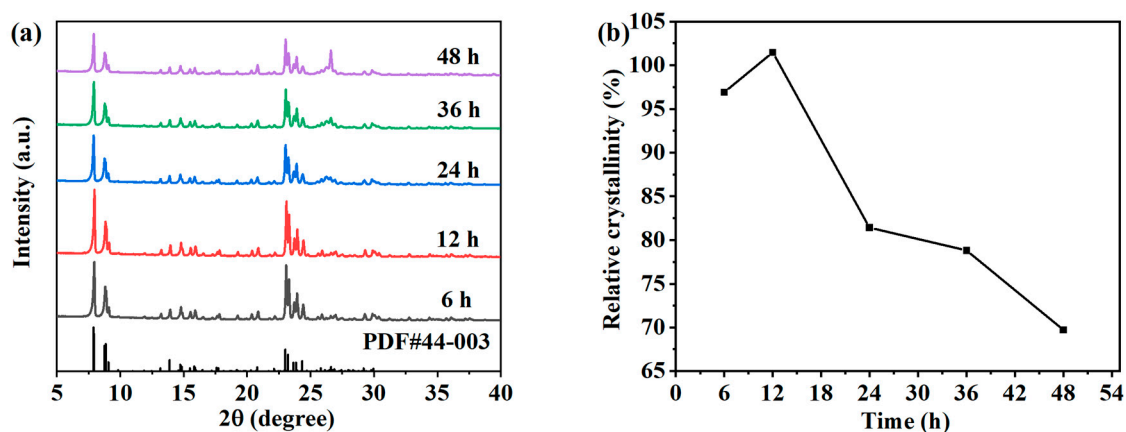


Figure 2. XRD patterns (a) and the relative crystallinity (b) of the ZSM-5 zeolites synthesized at different reaction times.

Figure 3a shows the adsorption and desorption isotherms of the ZSM-5 zeolites hydrothermally synthesized at different times under a N_2 atmosphere. The isotherm results show that the adsorption presents a typical Langmuir-I isotherm in the relative pressure range. The adsorption capacity of ZSM-5 zeolite in the N_2 atmosphere increased rapidly when $0.0 < P/P_0 < 0.1$, which was due to the adsorption in micropores. The pore size distribution in Figure 3b shows that ZSM-5 samples synthesized with different crystallization times are mainly composed of micropores [22]. The specific surface area, the pore size, and the pore volume of ZSM-5 zeolites crystallized within 6–48 h were shown in Table 2. When the crystallization time is 6 h and 12 h, the specific surface area is $335.16 \text{ m}^2 \cdot \text{g}^{-1}$ and $337.48 \text{ m}^2 \cdot \text{g}^{-1}$, respectively, and the pore volume is approximately $0.190 \text{ cm}^3 \cdot \text{g}^{-1}$. However, when the crystallization reaction time increases to 24 h, the specific surface area and the pore volume decrease to $244.59 \text{ m}^2 \cdot \text{g}^{-1}$ and $0.154 \text{ cm}^3 \cdot \text{g}^{-1}$, respectively; and at 48 h, the specific surface area and the pore volume decrease to $207.69 \text{ m}^2 \cdot \text{g}^{-1}$ and $0.131 \text{ cm}^3 \cdot \text{g}^{-1}$, respectively. In summary, since the specific surface area and the relative crystallinity of ZSM-5 zeolites are at a maximum at 12 h, this time is selected as the best crystallization time for the subsequent research in this work.

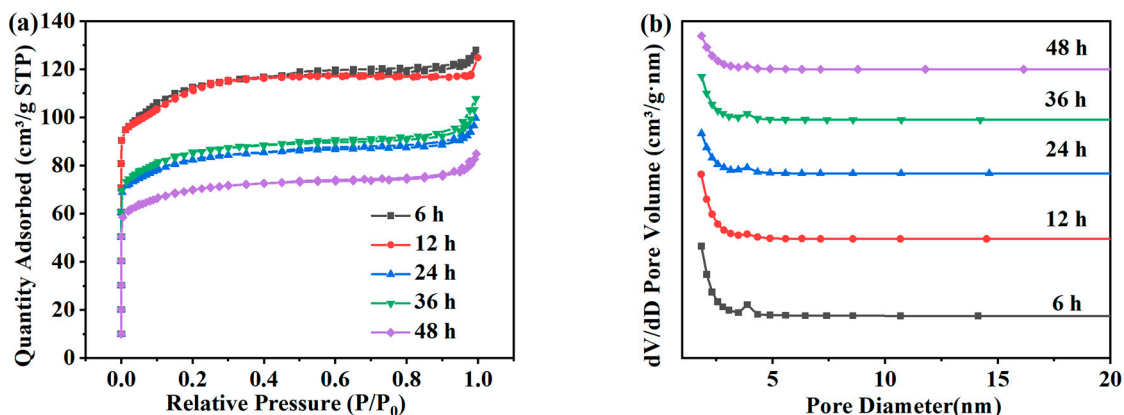


Figure 3. Adsorption and desorption isotherms (a) and pore size distribution (b) of ZSM-5 zeolites synthesized at different reaction times under a N₂ atmosphere.

Table 2. Pore structure parameters of ZSM-5 zeolites synthesized at different reaction times.

Time/(h)	S _{BET} /(m ² ·g ⁻¹)	S _{micro} /(m ² ·g ⁻¹)	S _{meso} /(m ² ·g ⁻¹)	V _{micro} /(cm ³ ·g ⁻¹)	V _{meso} /(cm ³ ·g ⁻¹)	V _{total} /(cm ³ ·g ⁻¹)	D _{pore} /(nm)
6	335.16	204.25	130.91	0.115	0.083	0.198	2.36
12	337.48	181.52	155.96	0.103	0.087	0.190	2.26
24	244.59	161.33	83.26	0.090	0.064	0.154	2.52
36	253.09	166.94	86.15	0.093	0.074	0.167	2.63
48	207.69	136.35	71.34	0.076	0.055	0.131	2.53

3.2. Effects of the Crystallization Reaction Temperature

In the preparation process of zeolite, the crystallization temperature has a significant impact on the crystallization reaction process of zeolite [23]. The appropriate crystallization reaction temperature can accelerate the dissolution of gel in the precursor, increase the ion concentration in the mixture, help the transformation of silicon aluminum gel to zeolite crystal, promote the formation and growth of crystal nucleus, and shorten the time required for crystallization. The effects of different synthesis temperatures on the hydrothermal crystallization of ZSM-5 zeolite were studied. The specific crystallization conditions were as follows: the crystallization time was 12 h, and the molar composition of SiO₂:Al₂O₃:Na₂O:H₂O:n-butyl amine is 1:0.005:0.2:30:0.4. XRD analysis (Figure 4a) shows that typical ZSM-5 peaks (7.9°, 8.8°, 23.0°, 23.9°, and 24.4°) exist in all the products obtained at 110–190 °C, indicating that ZSM-5 zeolites can be formed in this temperature range. As shown in Figure 4b, the relationship between the crystallization temperature and the relative crystallinity of each sample is represented by a broken line graph, which reflects that the relative crystallinity first increases and then decreases with the increase in the crystallization temperature. When the crystallization temperature is 110 °C, the diffraction peak strength of the product is very low, and the relative crystallinity is only 21.45%. When the crystallization temperature is too low, it is not conducive to the nucleation of ZSM-5 zeolite. If the crystallization degree is good, the required time needs to be greatly increased [24]. When the crystallization temperature was 130 °C, the diffraction peak strength and the relative crystallinity of the product increased greatly. As the crystallization temperature gradually increases, the characteristic peak intensity and the relative crystallinity of ZSM-5 zeolite show a slow and uniform increasing trend. When the crystallization reaction temperature is 170 °C, the relative crystallinity reaches a maximum of 101.47%. It can be seen that the appropriate temperature is conducive to the nucleation and crystallization of zeolite. However, when the crystallization reaction temperature further increased to 190 °C, the characteristic peak intensity decreased, the quartz phase was obviously formed, and the relative crystallinity decreased to 68.16%. Due to the high temperature, the growth

rate of the crystal is higher than the nucleation rate, which inhibits nucleation and also reduces the required preparation time. Therefore, in the subsequent time, the product is prone to transcrystallization, resulting in the formation of a heterocrystal, which reduces the purity of ZSM-5 zeolite.

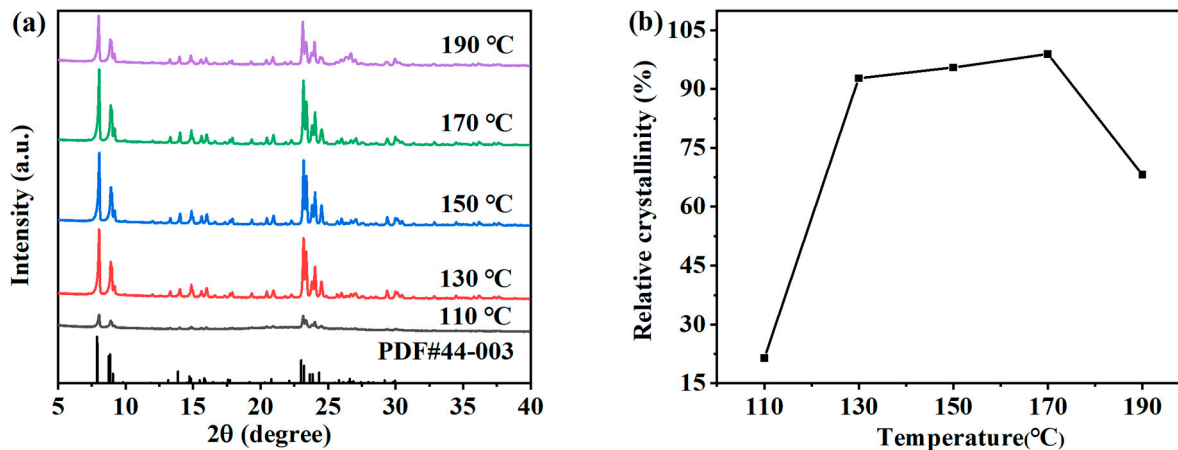


Figure 4. XRD patterns (a) and the relative crystallinity (b) of ZSM-5 zeolites synthesized at different reaction temperatures.

Figure 5a is the N_2 adsorption–desorption isotherms of the ZSM-5 zeolite samples prepared at different temperatures. The adsorption isotherms of ZSM-5 zeolites synthesized at 110 °C increased rapidly under high relative pressure ($P/P_0 = 0.6–1.0$), showing Langmuir-IV isotherms and H3 hysteresis loops, indicating that the products synthesized under these conditions were mainly mesoporous. Except for 110 °C, all ZSM-5 zeolites showed Langmuir-I isotherms. The adsorption capacity of ZSM-5 zeolites for N_2 shows a significant increase in the low-pressure region of $0.0 < P/P_0 < 0.1$, which is mainly due to the physical diffusion of N_2 molecules in the micropore structure of ZSM-5 zeolites. It shows that the sample is mainly composed of micropores. Figure 5b shows the pore size distribution. At 110 °C, there is a large pore volume at 5–6 nm, and at 130–190 °C, the pore structure of ZSM-5 zeolites prepared at 130–190 °C is mainly composed of micropores and a small number of mesopores. As shown in Table 3, the changing trend of the specific surface area and the pore volume is consistent with that of XRD. With the increase in temperature, the specific surface area and the pore volume increase first and then decrease. At 110 °C, although the product is a mesoporous structure and the average pore size reaches 11.10 nm, the specific surface area and the pore volume are only $267.45 \text{ m}^2 \cdot \text{g}^{-1}$ and $0.74 \text{ cm}^3 \cdot \text{g}^{-1}$ respectively due to the low crystallinity. At 130 °C, the specific surface area and the pore volume increase to $318.43 \text{ m}^2 \cdot \text{g}^{-1}$ and $0.185 \text{ cm}^3 \cdot \text{g}^{-1}$, respectively. When the temperature rises from 130 °C to 170 °C, the specific surface area and the pore volume further increase to $337.48 \text{ m}^2 \cdot \text{g}^{-1}$ and $0.190 \text{ cm}^3 \cdot \text{g}^{-1}$. However, at 190 °C, the pore structure performance decreases, and the specific surface area and the pore volume are only $234.08 \text{ m}^2 \cdot \text{g}^{-1}$ and $0.157 \text{ cm}^3 \cdot \text{g}^{-1}$, respectively. Therefore, based on the above analysis results, 170 °C was selected as the optimal hydrothermal synthesis reaction temperature.

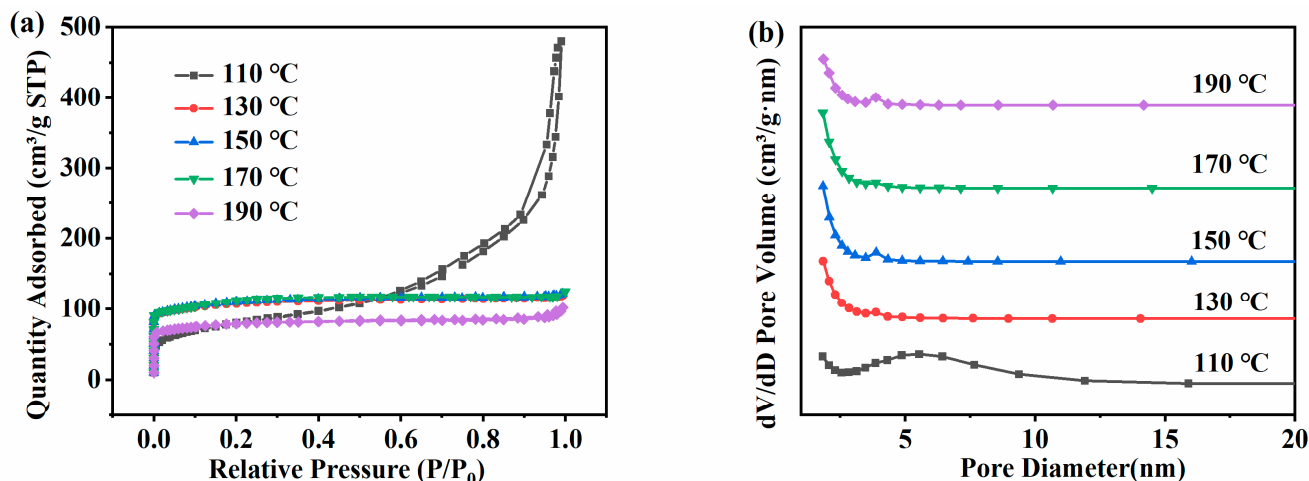


Figure 5. Adsorption and desorption isotherms (a) and pore size distribution (b) of ZSM-5 zeolites synthesized at different reaction temperatures under a N₂ atmosphere.

Table 3. Pore structure parameters of ZSM-5 zeolite synthesized at different temperatures.

Temperature/ (°C)	S _{BET} / (m ² ·g ⁻¹)	S _{micro} / (m ² ·g ⁻¹)	S _{meso} / (m ² ·g ⁻¹)	V _{micro} / (cm ³ ·g ⁻¹)	V _{meso} / (cm ³ ·g ⁻¹)	V _{total} / (cm ³ ·g ⁻¹)	D _{pore} / (nm)
110	267.45	48.13	219.32	0.027	0.713	0.74	11.10
130	318.43	213.79	104.64	0.119	0.066	0.185	2.33
150	330.07	208.66	121.41	0.116	0.072	0.188	2.28
170	337.48	181.52	155.96	0.103	0.087	0.190	2.26
190	234.08	147.97	86.11	0.083	0.074	0.157	2.68

3.3. Effects of the Na₂O/SiO₂ Molar Ratio

The pH value in the reaction system is also one of the important factors that directly affect the crystallization process of ZSM-5 zeolite. As an alkali metal cation, Na⁺ in the system can balance the skeleton charge, maintain the neutral charge of the skeleton, and play a certain structure-oriented role. The Na₂O/SiO₂ molar ratio determines whether the target product can be successfully prepared and controls the particle size of the zeolite. When the Na₂O/SiO₂ molar ratio is too high in the system, it is easy to generate impurity crystals. In order to clarify the effect of the Na₂O/SiO₂ molar ratio on the crystallization process of ZSM-5 zeolites, the precursor molar composition was changed: SiO₂:Al₂O₃:Na₂O:H₂O:n-butyl amine = 1:0.005:x:30:0.4 with x values of 0.05, 0.1, 0.2, 0.3 and 0.4, and the hydrothermal crystallization was conducted at 170 °C for 12 h. As shown in Figure 6a, XRD patterns of samples obtained under different Na₂O/SiO₂ molar ratios are shown. The obvious characteristic peaks of ZSM-5 zeolites in the figure indicate that the target product has been successfully synthesized, but the intensity of characteristic peaks decreases significantly when increasing to 0.3 and 0.4. The relative crystallinity of each product was calculated according to the XRD pattern. As shown in Figure 6b, the relative crystallinity first increased, then decreased with the increase in the molar ratio of Na₂O/SiO₂. When the Na₂O/SiO₂ molar ratio is 0.05, 0.1, and 0.2, the relative crystallinity is 97.20%, 102.71%, and 101.48%, respectively. The synthesized ZSM-5 zeolite has high purity. An appropriate alkaline solution environment can shorten the nucleation time of zeolites and accelerate the crystallization rate of zeolites. Excessive alkalinity may lead to the formation of impurity crystals. However, when the molar ratio of Na₂O/SiO₂ increases to 0.3 or 0.4, the relative crystallinity of the ZSM-5 zeolite was 86.71% or 68.76%, respectively. The excessive alkali concentration in the system will dissolve the metastable ZSM-5 zeolites in the system, thereby inhibiting the nucleation and growth of the crystal.

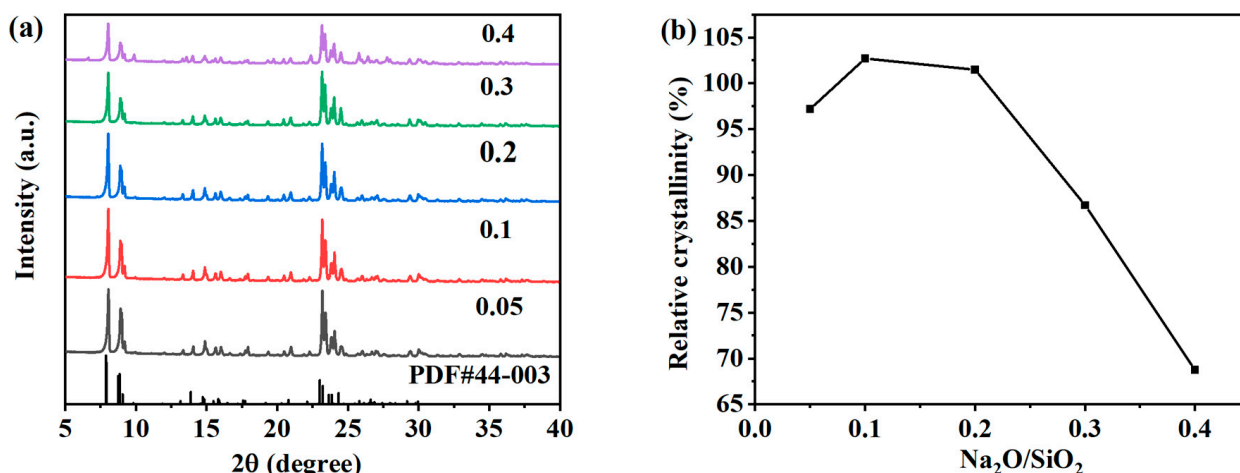


Figure 6. XRD patterns (a) and the relative crystallinity (b) of ZSM-5 zeolites synthesized at different Na₂O/SiO₂ molar ratios.

Figure 7a shows the adsorption and desorption isotherms and pore size distribution of ZSM-5 zeolites synthesized at different Na₂O/SiO₂ molar ratios under the N₂ atmosphere. The adsorption capacity of ZSM-5 zeolites for N₂ shows a significant increase in the low-pressure region of 0.0 < P/P₀ < 0.1, which is also mainly due to the physical diffusion of N₂ molecules in the micropore structure of ZSM-5 zeolites. And the adsorption capacity of N₂ shows a typical Langmuir-I isotherm. Figure 7b shows that the pore structure of ZSM-5 samples prepared at different Na₂O/SiO₂ molar ratios is mainly micropores. As shown in Table 4, when the molar ratio of Na₂O/SiO₂ increases from 0.05 to 0.1, the specific surface area increases from 295.81 m²·g⁻¹ to 321.94 m²·g⁻¹, and the specific surface area is the largest when the molar ratio of Na₂O/SiO₂ is 0.2, which is 337.48 m²·g⁻¹. Then increasing the molar ratio of Na₂O/SiO₂ in the system will not be conducive to the synthesis of ZSM-5 zeolite. The specific surface area of the product decreases to 305.12 m²·g⁻¹ when the molar ratio of Na₂O/SiO₂ increases to 0.4. In summary, because the relative crystallinity of ZSM-5 zeolites with Na₂O/SiO₂ molar ratios of 0.1 and 0.2 is similar, and the specific surface area at 0.2 is larger, 0.2 is selected as the optimal Na₂O/SiO₂ molar ratio.

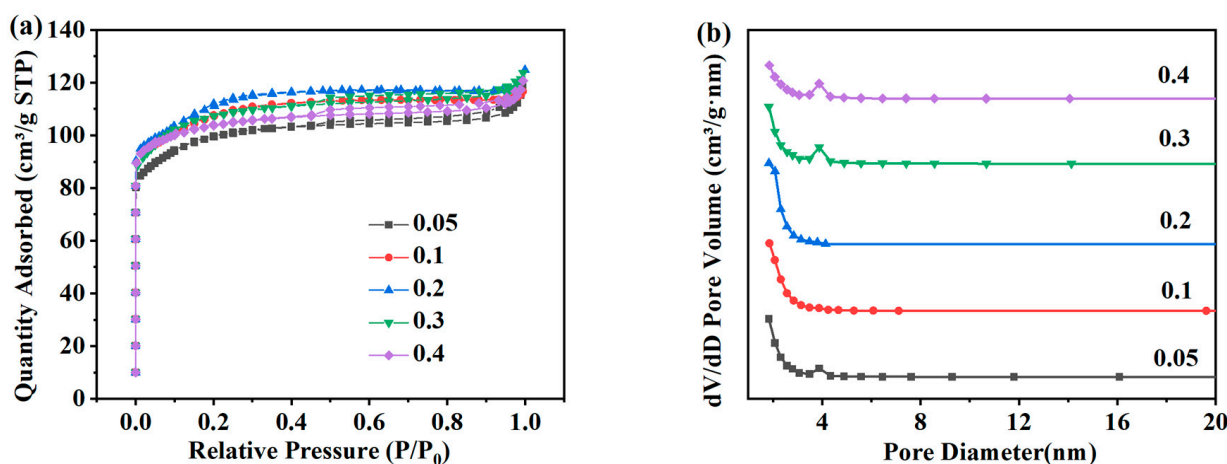


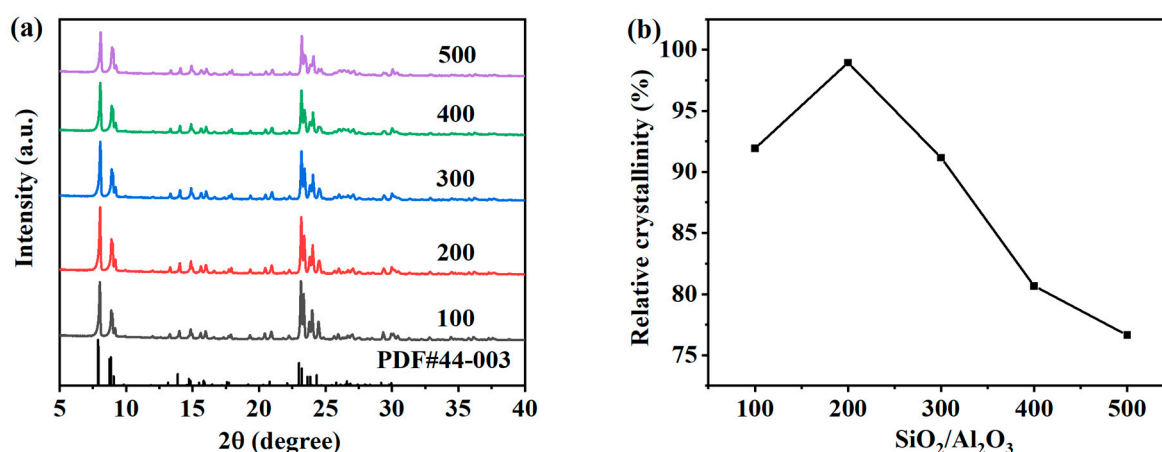
Figure 7. Adsorption and desorption isotherms (a) and pore size distribution (b) of ZSM-5 zeolites synthesized at different Na₂O/SiO₂ molar ratios under a N₂ atmosphere.

Table 4. Pore structure parameters of ZSM-5 zeolites synthesized at different Na₂O/SiO₂ molar ratios.

Na ₂ O/SiO ₂ Molar Ratio	S _{BET} / (m ² ·g ⁻¹)	S _{micro} / (m ² ·g ⁻¹)	S _{meso} / (m ² ·g ⁻¹)	V _{micro} / (cm ³ ·g ⁻¹)	V _{meso} / (cm ³ ·g ⁻¹)	V _{total} / (cm ³ ·g ⁻¹)	D _{pore} / (nm)
0.05	295.81	189.18	106.63	0.106	0.077	0.183	2.48
0.1	321.94	189.93	132.01	0.107	0.073	0.180	2.24
0.2	337.48	181.52	155.96	0.103	0.087	0.190	2.26
0.3	318.13	211.32	106.81	0.118	0.073	0.191	2.41
0.4	305.12	229.82	75.3	0.127	0.06	0.187	2.45

3.4. Effects of the SiO₂/Al₂O₃ Molar Ratio

The SiO₂/Al₂O₃ molar ratio is a key factor affecting the structure of ZSM-5 zeolite. In order to study the effect of the SiO₂/Al₂O₃ molar ratio, the values in SiO₂:Al₂O₃:Na₂O:H₂O:n-butylamine = 1:y:0.2:30:0.4 were 0.02, 0.01, 0.005, 0.003, 0.0025, and 0.002, respectively. SiO₂/Al₂O₃ molar ratios of 50, 100, 200, 300, 400, and 500 were studied, and hydrothermal crystallization was carried out at 170 °C for 12 h. Figure 8a shows the XRD spectrum of the product prepared by changing the molar ratio of the SiO₂/Al₂O₃ molar ratio, and the obvious five-finger peak indicates that the ZSM-5 zeolite was synthesized under different conditions. Figure 8b shows the relative crystallinity of each ZSM-5 zeolite corresponding to the XRD spectrum. The relative crystallinity shows the same trend as the characteristic peak intensity, which first increases and then decreases with the increase in the SiO₂/Al₂O₃ molar ratio. When the SiO₂/Al₂O₃ molar ratio increases from 100 to 200, the XRD characteristic diffraction peak intensity of the ZSM-5 zeolite sample gradually increases, and the relative crystallinity of the samples increases from 91.91% to 101.48%. The suitable SiO₂/Al₂O₃ molar ratio and the appropriate increase in silicate concentration in the system promoted the growth of ZSM-5 zeolite crystal nuclei [25]. With the further increase in the SiO₂/Al₂O₃ molar ratio, the crystallization rate of the zeolite gradually decreased. This is because aluminum can promote the growth of crystals, and the aluminum content in the system is reduced. When the molar ratio of SiO₂/Al₂O₃ further increased to 300, 400, and 500, the relative crystallinity of the samples gradually decreased to 91.17%, 80.66%, and 76.6%, respectively.

**Figure 8.** XRD patterns (a) and the relative crystallinity (b) of ZSM-5 zeolites synthesized at different SiO₂/Al₂O₃ molar ratios.

N₂ adsorption–desorption tests were carried out on ZSM-5 zeolites synthesized with different SiO₂/Al₂O₃ molar ratios, as shown in Figure 9a,b, which are the distributions of the specific surface area and pore size of the product. In Figure 5a, each product presents Langmuir-I isotherms within the range of relative pressure, and the samples are mainly composed of microporous structures. Table 5 lists the specific surface area, pore volume, and pore size of each ZSM-5 zeolite. The variation trend of the specific surface area is the

same as that of XRD. When the molar ratio of SiO₂/Al₂O₃ is 100, the specific surface area is 331.01 m²·g⁻¹. When the molar ratio of SiO₂/Al₂O₃ is 200, the pore structure is the best, the specific surface area increases to 337.48 m²·g⁻¹, and the pore volume is 0.190 cm³·g⁻¹. When the molar ratio of iO₂/Al₂O₃ is 300, the specific surface area and the pore volume of the samples decrease to 292.94 m²·g⁻¹ and 0.183 cm³·g⁻¹, respectively. When the molar ratio of SiO₂/Al₂O₃ increases to 500, the specific surface area and the pore volume decrease to 229.97 m²·g⁻¹ and 0.172 cm³·g⁻¹, respectively. Combined with the above analysis, 200 is selected as the optimal SiO₂/Al₂O₃ molar ratio.

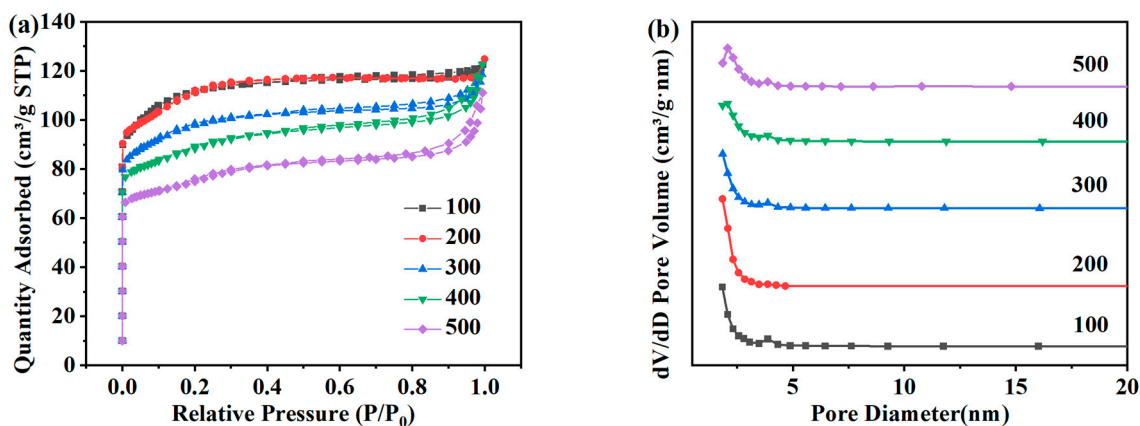


Figure 9. Adsorption and desorption isotherms (a) and pore size distribution (b) of ZSM-5 zeolites synthesized at different SiO₂/Al₂O₃ molar ratios under a N₂ atmosphere.

Table 5. Pore structure parameters of ZSM-5 zeolites synthesized at different SiO₂/Al₂O₃ molar ratios.

SiO ₂ /Al ₂ O ₃ Molar Ratio	S _{BET} / (m ² ·g ⁻¹)	S _{micro} / (m ² ·g ⁻¹)	S _{meso} / (m ² ·g ⁻¹)	V _{micro} / (cm ³ ·g ⁻¹)	V _{meso} / (cm ³ ·g ⁻¹)	V _{total} / (cm ³ ·g ⁻¹)	D _{pore} / (nm)
100	331.01	215.01	116	0.121	0.068	0.189	2.29
200	337.48	181.52	155.96	0.103	0.087	0.190	2.26
300	292.94	178.63	114.31	0.100	0.083	0.183	2.50
400	270.19	161.42	108.77	0.089	0.1	0.189	2.80
500	229.97	138.87	91.1	0.076	0.096	0.172	2.99

3.5. Composition and Structure Analysis of ZSM-5 Zeolites

The chemical content of the ZSM-5 zeolite is shown in Table 6. The results show that the actual SiO₂/Al₂O₃ molar ratio of the product is 104.93, which is a high silica–alumina ratio zeolite.

Table 6. Chemical content of the ZSM-5 zeolite prepared under optimum reaction conditions.

Component	SiO ₂ /(wt%)	Al ₂ O ₃ /(wt%)	Na ₂ O/(wt%)	SiO ₂ /Al ₂ O ₃ Molar Ratio	Na ₂ O/SiO ₂ Molar Ratio
Content	97.52	1.58	0.33	104.93	0.0033

Figure 10 is the SEM characterization of the ZSM-5 products prepared under optimal reaction conditions. It can be seen from the figures that the surface of the ZSM-5 zeolite samples is smooth, the morphology is complete and uniform, and it is a regular hexagonal prism structure, which conforms to the typical structure of ZSM-5 zeolite [26,27]. From the stacking structure of ZSM-5 zeolite samples, the grains are relatively complete, with a uniform distribution of grain sizes ranging from 1 to 4 μm.

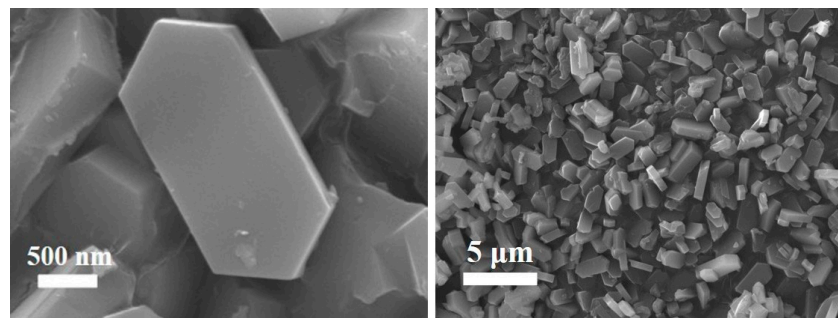


Figure 10. SEM images of ZSM-5 zeolite production.

Figure 11 is the TEM analysis results of the ZSM-5 products prepared under optimal reaction conditions. As shown in Figure 11, the zeolite is a hexagonal prism structure, which is consistent with the SEM analysis results. Figure 11b shows the distribution of Si, Al, O, and Na elements in ZSM-5 zeolite production. The results show that the distribution of each element is uniform, indicating that it is well embedded in the framework of zeolite. Figure 11c is the HR-TEM analysis result of ZSM-5 zeolite. The results show the clear lattice fringes of the particles. It can be seen that the crystal surface shows clear lattice fringes with a fringe spacing of 1.111 nm, which corresponds to the (101) lattice plane of ZSM-5 zeolite. The stripes with spacing of 1.093 nm correspond to the (011) lattice plane of ZSM-5 zeolite, and the stripes with spacing of 1.007 nm correspond to the (200) lattice plane of ZSM-5 zeolite. In the SAED diagram shown in Figure 11d, the arrangement of diffraction spots in two dimensions is periodic, and their distribution has obvious symmetry, indicating that the product is ZSM-5 zeolite with high crystallinity.

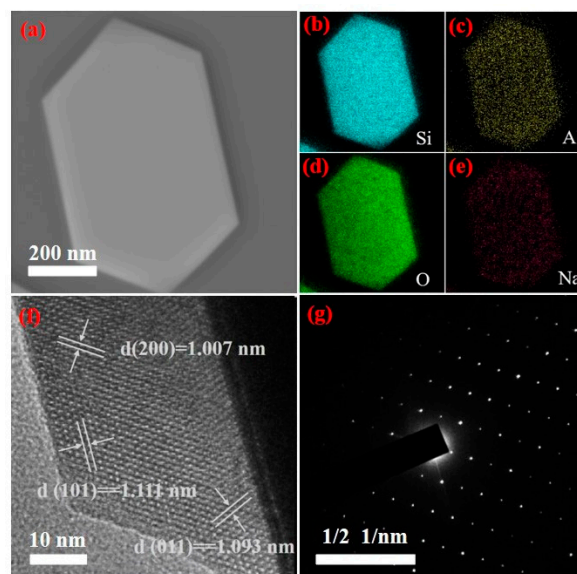


Figure 11. Transmission electron microscopy of ZSM-5 zeolite ((a) TEM diagram, (b–e) EDS diagram (Si, Al, O and Na), (f) HR-TEM diagram and (g) SAED diagram).

3.6. Static Adsorption Performance of ZSM-5 Zeolite for VOCs

p-xylene, benzene, toluene, and butyl acetate were used to evaluate the static adsorption performance of the ZSM-5 zeolite for VOCs. Figure 12 shows the saturated static adsorption capacity of the ZSM-5 molecular sieve for the above four organic compounds. The ZSM-5 zeolite sample showed good adsorption properties for p-xylene, benzene, toluene and butyl acetate, and the corresponding static saturation adsorption capacities were 118.85, 69.98, 68.74 and 95.85 $\text{mg}\cdot\text{g}^{-1}$, respectively. Figure 13 shows the FT-IR spectra of the ZSM-5 zeolite samples before and after static adsorption. The results show that the

characteristic peak near 450 cm^{-1} is the symmetric stretching vibration of the T-O-T (T is Si or Al) functional groups of $[\text{SiO}_4]$ and $[\text{AlO}_4]$ tetrahedrons [28]. The absorption peak at 545 cm^{-1} mainly represents the asymmetric stretching vibration of the five-membered ring structure functional groups in ZSM-5 zeolite [29]. The absorption peaks near 794 and 1099 cm^{-1} represent the bending vibration and asymmetric stretching vibration of the T-O-T functional groups (T is Si or Al) in the zeolite, respectively [30]. The characteristic absorption peak at 1224 cm^{-1} is caused by the asymmetric stretching vibration of the T-O-T bond of the zeolite MFI skeleton [31]. The absorption peaks at 3433 and 1600 cm^{-1} are the results of flexural vibration and tensile vibration of hydroxyl groups adsorbed water of ZSM-5 zeolites, respectively. Due to the low VOC content in the adsorbed ZSM-5 zeolite, this characteristic peak is not significant. The results show that the frequency band at 1099 cm^{-1} of the ZSM-5 zeolite samples saturated with different VOCs is wider than that of the unadsorbed sample. The bands at 700 and 733 cm^{-1} are attributed to the out-of-plane bending vibration of methyl in toluene. The peak at 1737 cm^{-1} is the result of the stretching vibration of $-\text{C}=\text{O}$, the 2878 cm^{-1} band corresponds to the symmetric stretching vibration of butyl acetate methyl, and the 2980 cm^{-1} band belongs to the antisymmetric stretching vibration of methyl.

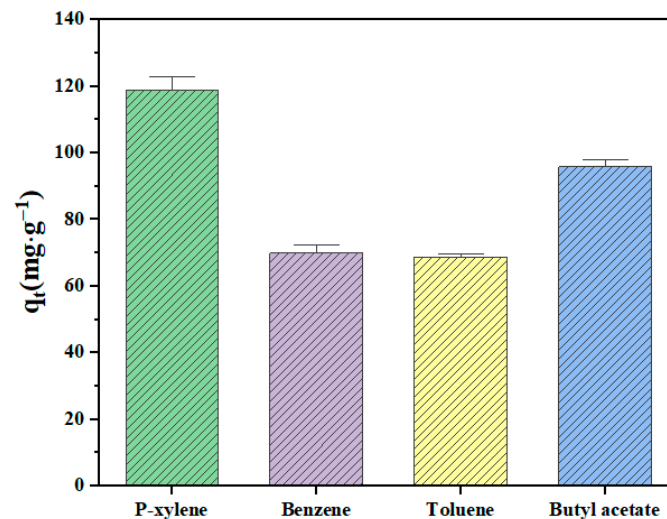


Figure 12. Static adsorption capacity of VOCs on ZSM-5 zeolite.

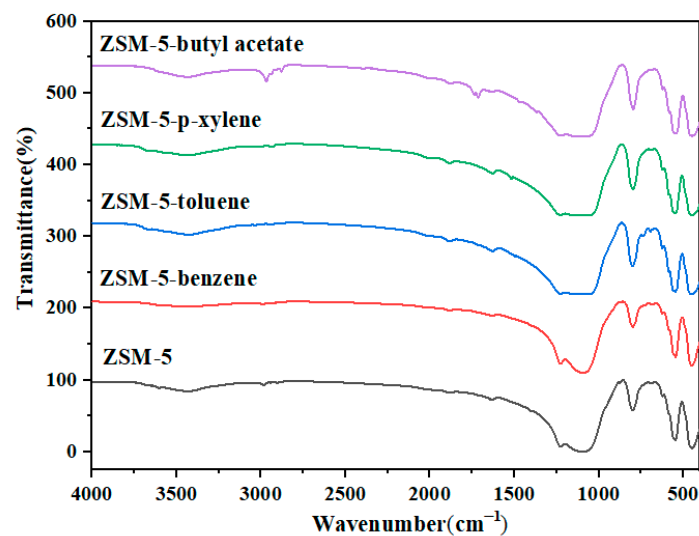


Figure 13. Infrared spectra of ZSM-5 zeolite before and after static adsorption of VOCs.

4. Conclusions

In summary, we provide a method to prepare ZSM-5 zeolite for VOCs adsorption by controlled one-step hydrothermal crystallization by using coal gasification slag desilication liquid as the main silicon and sodium sources, mixing with an aluminum source, template agent and ZSM-5 zeolite seed without the aging step, and verify the static adsorption effect of samples on four VOCs. This method will help to realize the high-value utilization of solid waste silicon resources, and provide a new means to solve air pollutants by using solid waste. ZSM-5 zeolites were prepared by a hydrothermal method with desilication solution as the main raw material, by controlling the hydrothermal crystallization temperature, time, the $\text{Na}_2\text{O}/\text{SiO}_2$ molar ratio, and the $\text{SiO}_2/\text{Al}_2\text{O}_3$ molar ratio. The optimum synthesis conditions were as follows: the hydrothermal crystallization temperature was 170 °C, the reaction time was 12 h, the $\text{Na}_2\text{O}/\text{SiO}_2$ molar ratio was 0.2, and the $\text{SiO}_2/\text{Al}_2\text{O}_3$ molar ratio was 200. Under the optimal conditions, the ZSM-5 zeolite was prepared with a relative crystallization of 101.48%, a specific surface area of $337.48 \text{ m}^2 \cdot \text{g}^{-1}$, and a pore volume of $0.190 \text{ cm}^3 \cdot \text{g}^{-1}$. The morphology of ZSM-5 zeolite is a regular hexagonal prism structure, with uniform distribution between crystal particles and high crystallinity. The static saturated adsorption capacities of ZSM-5 zeolite prepared under the optimal conditions for benzene, toluene, p-xylene and butyl acetate were 69.98, 68.74, 118.85, and 95.85 $\text{mg} \cdot \text{g}^{-1}$, respectively, indicating that the prepared ZSM-5 zeolite can be effectively used to adsorb VOCs pollutants. With the increase in the utilization of coal gasification slag and the extensive demand for the treatment of VOCs pollutants, the preparation of ZSM-5 zeolite products will have significant industry demand.

Author Contributions: Conceptualization, C.W. and H.L.; methodology, Z.H. and Q.S.; software, Q.S.; validation, J.Z., Z.H. and S.L.; formal analysis, G.Z.; investigation, Q.S.; resources, Z.S.; data curation, G.Z.; writing—original draft preparation, Q.S. and Q.Z.; writing—review and editing, S.L., Q.Z. and Z.S.; visualization, Z.S. and Q.S.; supervision, Q.Z.; project administration, C.W.; funding acquisition, Z.S. All authors have read and agreed to the published version of the manuscript.

Funding: This research was funded by the National Key R&D Program of China (2021YFC2903203), the National Natural Science Foundation of China (No. 52204425), and the Youth Innovation Promotion Association CAS (2021045).

Data Availability Statement: The data presented in this study are available on request from the corresponding author.

Conflicts of Interest: The authors declare no conflict of interest.

References

1. Bensafi, B.; Chouat, N.; Djafri, F. The universal zeolite ZSM-5: Structure and synthesis strategies. A review. *Coord. Chem. Rev.* **2023**, *496*, 215397. [[CrossRef](#)]
2. Miyake, K.; Inoue, R.; Miura, T.; Nakai, M.; Al-Jabri, H.; Hirota, Y.; Uchida, Y.; Tanaka, S.; Miyamoto, M.; Inagaki, S.; et al. Improving hydrothermal stability of acid sites in MFI type aluminosilicate zeolite (ZSM-5) by coating MFI type all silica zeolite (silicalite-1) shell layer. *Microporous Mesoporous Mater.* **2019**, *288*, 109523. [[CrossRef](#)]
3. Su, X.; Zhang, K.; Sntenkova, Y.; Matieva, Z.; Bai, X.; Kolesnichenko, N.; Wu, W. High-efficiency nano [Zn,Al]ZSM-5 bifunctional catalysts for dimethyl ether conversion to isoparaffin-rich gasoline. *Fuel Process. Technol.* **2020**, *198*, 106242. [[CrossRef](#)]
4. Wang, F.; Chu, X.; Zhao, P.; Zhu, F.; Li, Q.; Wu, F.; Xiao, G. Shape selectivity conversion of biomass derived glycerol to aromatics over hierarchical HZSM-5 zeolites prepared by successive steaming and alkaline leaching: Impact of acid properties and pore constraint. *Fuel* **2020**, *262*, 116538. [[CrossRef](#)]
5. Al-Jubouri, S.M.; Al-Batty, S.I.; Holmes, S.M. Using the ash of common water reeds as a silica source for producing high purity ZSM-5 zeolite microspheres. *Microporous Mesoporous Mater.* **2021**, *316*, 110953. [[CrossRef](#)]
6. Lauridant, N.; Daou, T.J.; Arnold, G.; Soulard, M.; Nouali, H.; Patarin, J.; Faye, D. Key steps influencing the formation of ZSM-5 films on aluminum substrates. *Microporous Mesoporous Mater.* **2012**, *152*, 1–8. [[CrossRef](#)]
7. Qi, T.; Teng, J.; Shi, J.; Chu, G.; Zou, H.; Luo, Y.; Zhang, L.; Sun, B. Synthesis of ZSM-5 zeolite by dynamic hydrothermal method with premixing in the rotating packed bed: An process mechanism analysis. *Chem. Ind. Eng. Prog.* **2021**, *40*, 6228–6234.
8. Jafari, S.; Ghorbani-Shahna, F.; Bahrami, A.; Kazemian, H. Adsorptive removal of toluene and carbon tetrachloride from gas phase using Zeolitic Imidazolate Framework-8: Effects of synthesis method, particle size, and pretreatment of the adsorbent. *Microporous Mesoporous Mater.* **2018**, *268*, 58–68. [[CrossRef](#)]

9. Wu, S.; Wang, Y.; Sun, C.; Zhao, T.; Zhao, J.; Wang, Z.; Liu, W.; Lu, J.; Shi, M.; Zhao, A.; et al. Novel preparation of binder-free Y/ZSM-5 zeolite composites for VOCs adsorption. *Chem. Eng. J.* **2021**, *417*, 129172. [[CrossRef](#)]
10. Yang, C.; Miao, G.; Pi, Y.; Xia, Q.; Wu, J.; Li, Z.; Xiao, J. Abatement of various types of VOCs by adsorption/catalytic oxidation: A review. *Chem. Eng. J.* **2019**, *370*, 1128–1153. [[CrossRef](#)]
11. Yuan, N.; Zhao, A.; Hu, Z.; Tan, K.; Zhang, J. Preparation and application of porous materials from coal gasification slag for wastewater treatment: A review. *Chemosphere* **2022**, *287*, 132227. [[CrossRef](#)]
12. Qu, J.; Zhang, J.; Sun, Z.; Yang, C.; Shi, D.; Li, S.; Li, H. Research progress on comprehensive utilization of coal gasification slag. *Clean Coal Technol.* **2020**, *26*, 10–18.
13. Chang, S.; Zhuo, J.; Meng, S.; Qin, S.; Yao, Q. Clean Coal Technologies in China: Current Status and Future Perspectives. *Engineering* **2016**, *2*, 447–459. [[CrossRef](#)]
14. Wu, S.; Huang, S.; Wu, Y.; Gao, J. Characteristics and catalytic actions of inorganic constituents from entrained-flow coal gasification slag. *J. Energy Inst.* **2015**, *88*, 93–103. [[CrossRef](#)]
15. Zhang, J.; Zuo, J.; Jiang, Y.; Zhu, D.; Zhang, J.; Wei, C. Kinetic analysis on the mesoporous formation of coal gasification slag by acid leaching and its thermal stability. *Solid State Sci.* **2020**, *100*, 106084. [[CrossRef](#)]
16. Qu, J.; Zhang, J.; Li, H.; Li, S. A high value utilization process for coal gasification slag: Preparation of high modulus sodium silicate by mechano-chemical synergistic activation. *Sci. Total Environ.* **2021**, *801*, 149761. [[CrossRef](#)] [[PubMed](#)]
17. Xue, T.; Liu, H.; Zhang, Y.; Wu, H.; Wu, P. Synthesis of ZSM-5 with hierarchical porosity: In-situ conversion of the mesoporous silica-alumina species to hierarchical zeolite. *Microporous Mesoporous Mater.* **2017**, *242*, 190–199. [[CrossRef](#)]
18. Al-Jubouris, M. Synthesis of hierarchically porous ZSM-5 zeolite by self-assembly induced by aging in the absence of seeding-assistance. *Microporous Mesoporous Mater.* **2020**, *303*, 110296. [[CrossRef](#)]
19. GAao, J.; Wang, W.; Zhang, J.; Lei, Z.; Shi, D.; Qu, L. Study on synthesis and adsorption performance of hydrophobic ZSM-5 zeolites for removal of toluene in high-humidity exhaust gas. *J. Chem. Ind. Eng.* **2020**, *71*, 337–343.
20. Huang, X.; Wang, C.; Zhu, Y.; Xu, W.; Sun, Q.; Xing, A.; Ma, L.; Li, J.; Han, Z.; Wang, Y. Facile synthesis of ZSM-5 nanosheet arrays by preferential growth over MFI zeolite [100] face for methanol conversion. *Microporous Mesoporous Mater.* **2019**, *288*, 109573. [[CrossRef](#)]
21. Bai, R.; Sun, Q.; Song, Y.; Wang, N.; Zhang, T.; Wang, F.; Zou, Y.; Feng, Z.; Miao, S.; Yu, J. Intermediate-crystallization promoted catalytic activity of titanasilicate zeolites. *J. Mater. Chem. A* **2018**, *6*, 8757–8762. [[CrossRef](#)]
22. Li, X.; Wang, J.; Guo, Y.; Zhu, T.; Xu, W. Adsorption and desorption characteristics of hydrophobic hierarchical zeolites for the removal of volatile organic compounds. *Chem. Eng. J.* **2021**, *411*, 128558. [[CrossRef](#)]
23. Mohiuddin, E.; Isa, Y.M.; Mdleleni, M.M.; Sincadu, N.; Key, D.; Tshabalala, T. Synthesis of ZSM-5 from impure and beneficiated Grahamstown kaolin: Effect of kaolinite content, crystallisation temperatures and time. *Appl. Clay Sci.* **2016**, *119*, 213–221. [[CrossRef](#)]
24. Kimj, K.; Leeh, D. Effects of step change of heating source on synthesis of zeolite 4A from coal fly ash. *J. Ind. Eng. Chem.* **2009**, *15*, 736–742.
25. Cheng, Y.; Liao, R.H.; Li, J.S.; Sun, X.Y.; Wang, L.J. Synthesis research of nanosized ZSM-5 zeolites in the absence of organic template. *J. Mater. Process. Technol.* **2008**, *206*, 445–452. [[CrossRef](#)]
26. Sun, Y.; Ma, T.; Cao, S.; Wang, J.; Meng, X.; Gong, Y.; Zhang, Z.; Ma, A.; Liu, P. Defective sites in ZSM-5 zeolite synthesized by n-butylamine template facilitating uniform meso-microporosity by alkali-treatment. *Microporous Mesoporous Mater.* **2021**, *326*, 111360. [[CrossRef](#)]
27. Kadja, G.T.M.; Suprianti, T.R.; Ilmi, M.M.; Khalil, M.; Mukti, R.R.; Subagjo. Sequential mechanochemical and recrystallization methods for synthesizing hierarchically porous ZSM-5 zeolites. *Microporous Mesoporous Mater.* **2020**, *308*, 110550. [[CrossRef](#)]
28. Ismail, A.A.; Mohamed, R.M.; Fouad, O.A.; Ibrahim, I.A. Synthesis of nanosized ZSM-5 using different alumina sources. *Cryst. Res. Technol.* **2006**, *41*, 145–149. [[CrossRef](#)]
29. Jiang, T.; Wang, F.; Zhang, X.; Zhai, Y.; Lv, G.; Shen, Y.; Wu, Y. Facile synthesis of ZSM-5 mesocrystal via novel pathway of crystallization: Fast precipitation, deconstruction and reorganization. *Microporous Mesoporous Mater.* **2021**, *321*, 111112. [[CrossRef](#)]
30. Hamid, S.; Kumar, M.A.; Lee, W. Highly reactive and selective Sn-Pd bimetallic catalyst supported by nanocrystalline ZSM-5 for aqueous nitrate reduction. *Appl. Catal. B Environ.* **2016**, *187*, 37–46. [[CrossRef](#)]
31. Xie, Y.; Cao, H.; Li, Y.; Zhang, Y.; Crittenden, J.C. Highly selective PdCu/amorphous silica-alumina (ASA) catalysts for groundwater denitration. *Environ. Sci. Technol.* **2011**, *45*, 4066–4072. [[CrossRef](#)] [[PubMed](#)]

Disclaimer/Publisher's Note: The statements, opinions and data contained in all publications are solely those of the individual author(s) and contributor(s) and not of MDPI and/or the editor(s). MDPI and/or the editor(s) disclaim responsibility for any injury to people or property resulting from any ideas, methods, instructions or products referred to in the content.